THEORETICAL INVESTIGATION OF THE THERMOCHEMICAL DEGRADATION OF GRAPHITE IN A HIGH-ENTHALPY AIR FLOW

A. G. Gofman and A. M. Grishin

UDC 536.24

Ablating materials are widely used for organizing the thermal shielding of hypersonic vehicles. In particular, graphite is often used for this purpose. The thermochemical degradation of an ablator in a hypersonic flow is a very complex process, since it is necessary to take into account not only the sublimation of the material but also various heterogeneous and homogeneous nonequilibrium chemical reactions.

The results of a series of experimental investigations of the physicochemical processes of interaction between high-enthalpy air and a graphite surface are summarized in [1, 2], which give the characteristics of the more important heterogeneous reactions [1] and the nonequilibrium sublimation of the graphite [2].

A theoretical investigation of the interaction of high-enthalpy air and graphite can be found in studies [3-10]. Whereas in [3] it is assumed that the chemical reactions in the flow are "frozen," in [4-8] they are assumed to be "equilibrium." In [4, 6] the effect of multicomponent diffusion on the characteristics of the process is investigated. In [5] the rate and temperature of ablation are compared with those determined in [3] and good agreement is noted. In [7] the investigation is based on the assumption of equilibrium sublimation of the graphite from the surface in the form of atomic carbon. The transition of the heterogeneous graphite oxidation process from the kinetic to the diffusion regime, depending on the value of the kinetic constants of the heterogeneous reaction, is studied in [8]. The interaction of graphite and a nonequilibrium oxygen or air flow was systematically investigated in [9]. However, the data on the heterogeneous reactions used in [9] do not reflect the effect of the degree of dissociation of O_2 on the rate of erosion of the graphite, which, according to [1], seriously distorts its value. In [10] certain results relating to the interaction of a high-enthalpy nonequilibrium air flow and a graphite surface are presented and compared with the model of a "frozen" boundary layer; however, in this study, as in [9], the components C_2 and C_3, which are important in the graphite sublimation regime, are not taken into account.

As follows from the analysis given in [11, 12], at present there is no satisfactory agreement between the theoretical and experimental data on the thermochemical degradation of graphite, which is attributable to the limitations of the theoretical models.

Below, we present a mathematical model of the thermochemical degradation of graphite in a hypersonic flow that takes into account the more important nonequilibrium physicochemical processes that occur when graphite interacts with a dissociated air flow. The principal interaction regimes: kinetic, diffusion, and sublimation, are examined. The results of calculating the characteristics of the process in accordance with the model proposed are compared with the results obtained using the simpler models of an "equilibrium" or "frozen" boundary layer, both in the neighborhood of the stagnation point and along the generator of the body of revolution. It is shown that of the simplified models the equilibrium boundary layer approximation is the more accurate, although even in this case the error in determining the heat flux and the ablation rate of the lateral surface of the body may reach 25%. The theoretical and experimental results are compared and it is shown that when the mathematical model that takes the nonequilibrium physicochemical processes into account is used they are in satisfactory agreement.

1. Formulation of the Problem and Method of Solution

We will consider the problem of an axisymmetric graphite body of given shape in a high-enthalpy laminar air flow at zero angle of attack. The excitation of all the internal degrees of freedom of the chemical components is assumed to be equilibrium, and the investigation is carried out in the flow regime where the ionization and radiation of the gas can be

Tomsk. Translated from Zhurnal Prikladnoi Mekhaniki i Tekhnicheskoi Fiziki, No. 4, pp. 107-114, July-August, 1984. Original article submitted May 4, 1983.

0021-8944/84/2504-0598$08.50

disregarded. The gas mixture is regarded as a mixture of perfect gases, and in describing the diffusion properties of the multicomponent mixture the effect of thermal diffusion is neglected. The surface of the body is assumed to be smooth.

For sufficiently large Reynolds numbers this process is mathematically described by the system of equations of a multicomponent, chemically nonequilibrium laminar layer, which in Dorodnitsyn–Lees type variables takes the form

$$\frac{\partial}{\partial\eta}\left(l\frac{\partial\tilde{u}}{\partial\eta}\right)+f\frac{\partial\tilde{u}}{\partial\eta}=\beta\left(\tilde{u}^2-\rho_e/\rho\right)+\alpha\left(\tilde{u}\frac{\partial\tilde{u}}{\partial s}-\frac{\partial f}{\partial s}\frac{\partial\tilde{u}}{\partial\eta}\right); \tag{1.1}$$

$$-\frac{\partial X_i}{\partial\eta}+f\frac{\partial c_i}{\partial\eta}=\alpha\left(\tilde{u}\frac{\partial c_i}{\partial s}-\frac{\partial f}{\partial s}\frac{\partial c_i}{\partial\eta}\right)-a_1\frac{W_i}{\rho},\quad i=\overline{1,L_k}; \tag{1.2}$$

$$-\frac{\partial X_i^*}{\partial\eta}+f\frac{\partial c_i^*}{\partial\eta}=\alpha\left(\tilde{u}\frac{\partial c_i^*}{\partial s}-\frac{\partial f}{\partial s}\frac{\partial c_i^*}{\partial\eta}\right),\quad i=\overline{L_{k+1},L-1}; \tag{1.3}$$

$$\frac{\partial}{\partial\eta}\left(\frac{l}{\mathrm{Pr}}\frac{\partial H}{\partial\eta}\right)+f\frac{\partial H}{\partial\eta}+\frac{\partial}{\partial\eta}\left[l\left(1-\frac{1}{\mathrm{Pr}}\right)\frac{\partial}{\partial\eta}\left(\frac{\tilde{u}^2}{2}\right)\right]=\alpha\left(\tilde{u}\frac{\partial H}{\partial s}-\frac{\partial f}{\partial s}\frac{\partial H}{\partial\eta}\right)+$$
$$+\frac{\partial}{\partial\eta}\left[\sum_{i=1}^{L_k}\tilde{h}_i\left(X_i+\frac{l}{\mathrm{Pr}}\frac{\partial c_i}{\partial\eta}\right)+\sum_{i=L_{k+1}}^{L}h_i\left(X_i^*+\frac{l}{\mathrm{Pr}}\frac{\partial c_i^*}{\partial\eta}\right)\right]; \tag{1.4}$$

$$\sum_{j=1}^{L_k}a_{ij}X_j+\sum_{j=L_{k+1}}^{L}a_{ij}X_j^*=l\left(\sum_{j=1}^{L_k}b_{ij}\frac{\partial c_j}{\partial\eta}+\sum_{j=L_{k+1}}^{L}b_{ij}\frac{\partial c_j^*}{\partial\eta}\right),\quad i=\overline{1,L-1}; \tag{1.5}$$

$$\sum_{i=L_{k+1}}^{L}X_i^*=0,\quad \sum_{i=L_{k+1}}^{L}c_i^*=1; \tag{1.6}$$

$$p_e=\rho RT/M. \tag{1.7}$$

This system of equations must be solved for the following boundary conditions:

$$\tilde{u}\,|_{\eta=0}=0; \tag{1.8}$$

$$f\,|_{\eta=0}=f_w; \tag{1.9}$$

$$-X_{iw}+\left(f_w+\alpha\frac{df_w}{ds}\right)c_{iw}=-R_ia_2,\quad i=\overline{1,L_k}; \tag{1.10}$$

$$-X_{iw}^*+\left(f_w+\alpha\frac{df_w}{ds}\right)c_{iw}^*=-R_i^*a_2,\quad i=\overline{L_{k+1},L-1}; \tag{1.11}$$

$$T\,|_{\eta=0}=T_w; \tag{1.12}$$

$$\tilde{u}\,|_{\eta\to+\infty}=1; \tag{1.13}$$

$$c_i|_{\eta\to+\infty}=c_{ie},\quad i=\overline{1,L_k}; \tag{1.14}$$

$$c_i^*|_{\eta\to+\infty}=c_{ie}^*,\quad i=\overline{L_{k+1},L-1}; \tag{1.15}$$

$$H\,|_{\eta\to+\infty}=H_e. \tag{1.16}$$

The boundary conditions for system (1.1)-(1.7) at s = 0 are the equations of the self-similar boundary layer obtained from that system. For determining the value of the characteristics of the external inviscid flow over the surface of the body we use the conservation equations along the streamline for a given distribution $p_e(s)$:

$$\rho_e u_e du_e/ds=-dp_e/ds; \tag{1.17}$$

$$\rho_e u_e dc_{ie}/ds=R_N W_{ie},\quad i=\overline{1,L_k}; \tag{1.18}$$

$$c_{ie}^*=c_{ie0}^*,\quad i=\overline{L_{k+2},L-1}; \tag{1.19}$$

$$H_e = H_{e0}; \tag{1.20}$$

$$p_e = \rho_e R T_e / M_e. \tag{1.21}$$

Here and above, x and y are the independent variables of the natural orthogonal coordinate system tied to the surface of the body; r, the distance from a point in the flow to the axis of symmetry; $\eta = \left(u_e r \int_0^y \rho dy\right) \Big/ \sqrt{2\xi}$; $\xi = \int_0^x \rho_e u_e \mu_e r^2 dx$; $s = x/R_N$; $\tilde{u} = u/u_e$; u, the tangential component of the velocity vector; H, the total enthalpy in the gas flow; $L_k = L - N_e$; N_e, the number of independent chemical components and the total number of components of the mixture; $c_i^* = c_i + \sum_{k=1}^{L_k} \nu_{ki} \frac{m_i}{m_k} c_k$, $i = \overline{L_{k+1}, L}$ the concentration of the i-th chemical element; $\{\nu_{ki}\}$, the stoichiometric matrix, whose construction is described in [13]; J_i^*, the diffusion flux of the i-th element [13]; $\tilde{h}_i = h_i - \sum_{k=L_{k+1}}^{L} h_k \nu_{ik} \frac{m_k}{m_i}$, $i \leqslant L_k$; R_i, W_i the rate of formation of the i-th component as a result of the heterogeneous and homogeneous reactions, respectively; $R_i^* = R_i + \sum_{k=1}^{L_k} \nu_{ki} \frac{m_i}{m_k} R_k$; R_N, the radius of curvature of the surface at the stagnation point; $X_i = J_i a_2$; $a_2 = \sqrt{a_1/(\rho_e \mu_e)}$; $a_1 = 2\xi/(u_e \xi_x')$; $\alpha = 2\xi/\xi_s'$; $\beta = \alpha/u_e \frac{du_e}{ds}$; f_w is determined from the relation $f_w + \alpha df_w/ds = -(\rho v)_w a_2$; the functions p, T, M, μ, ρ, l, f, c_i, J_i, m_j, h_i, S_{ij}, D_{ij}, Pr, λ, c_p, $(\rho v)_w$, α_{ij}, b_{ij} are given in [10]; the subscripts w, e, 0, ∞ are assigned to quantities at the surface of the body, at the outer edge of the boundary layer, on the axis of symmetry, and in the free stream, respectively.

Equation (1.1) is a corollary of the equations of continuity and conservation of momentum in the direction of the x axis, Eq. (1.2) is the law of mass conservation for the component, and (1.3) that for the element; Eq. (1.4) is the law of energy conservation, and (1.5) are the Stefan–Maxwell relations in the form proposed in [14]. Relations (1.6) are the algebraic integrals of the system of equations of the multicomponent boundary layer.

An analysis of the experimental data [1, 2] shows that it is necessary to take the following mixture components into account; O_2(1), N_2(2), NO(3), CO_2(4), CO(5), CN(6), C_2(7), C_3(8), C(9), O(10), N(11) (the number in parentheses is the number of the chemical component). At the surface of the graphite the following heterogeneous reactions take place:

$$C_{SO} + O_2 \to 2CO, \quad C_{SO} + O \to CO, \quad O + O \to O_2, \tag{1.22}$$

where C_{SO} stands for graphite in the solid phase.

With respect to the other components the surface is assumed to be neutral. The data on the heterogeneous reactions are taken from [1]. Sublimation from the surface of the graphite is assumed to involve the components C, C_2, C_3:

$$C_{SO} \rightleftarrows C, \quad C_{SO} \rightleftarrows C_2, \quad C_{SO} \rightleftarrows C_3. \tag{1.23}$$

The data on the saturated vapor pressure C, C_2, and C_3 are taken from [2]. In the flow we have the nonequilibrium chemical reactions:

$$\begin{array}{llll}
N_2 + M \rightleftarrows 2N + M & (1), & NO + M \rightleftarrows N + O + M & (2), \\
O_2 + M \rightleftarrows 2O + M & (3), & N_2 + O \rightleftarrows NO + N & (4), \\
NO + O \rightleftarrows O_2 + N & (5), & CO_2 + M \rightleftarrows CO + O + M & (6), \\
CO + M \rightleftarrows C + O + M & (7), & CN + M \rightleftarrows C + N + M & (8), \\
C_3 + M \rightleftarrows 3C + M & (9), & C_2 + M \rightleftarrows 2C + M & (10), \\
N_2 + C \rightleftarrows CN + N & (11), & CO + N \rightleftarrows CN + O & (12), \\
CN + O \rightleftarrows C + NO & (13), & CO + N \rightleftarrows NO + C & (14), \\
CO_2 + O \rightleftarrows CO + O_2 & (15), & C_2 + O \rightleftarrows CO + C & (16), \\
C_3 + O \rightleftarrows CO + C_2 & (17). &&
\end{array} \tag{1.24}$$

Here, M is a catalyst, which may be any component of the mixture. The numbers in parentheses are the numbers of the reactions. The constants of the direct reactions (1)-(8), (11)-(15) are taken from [15]. The transfer coefficients μ, λ, D_{ij} were calculated in the same way as in [10]. All the thermodynamic quantities were calculated on the basis of the approximations given in [16]. As the dependent chemical components we took O_2, N_2, NO_2, CO_2, CO, CN, C_2, C_3

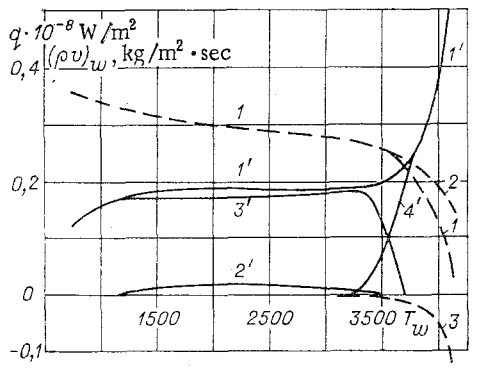

Fig. 1

and as the independent homogeneous chemical reactions dissociation reactions (1)-(3), (6)-(10) from (1.24). The elemental composition of the air was taken to be as follows: $c^*_{e,O} = 0.236567$, $c^*_{e,O} = 0$, $c^*_{e,N} = 1 - c^*_{e,O}$. The accommodation coefficients α_i for the components C, C_2, and C_3 are equal to 0.24, 0.5, and 0.09 respectively. It was not possible to find published data on the thermokinetic constants of nonequilibrium reactions (9), (10), (16), (17) from (1.24). In the calculations they were taken equal to $k_9 = k_{10} = 39$, $n_9 = n_{10} = -1$, $E_9 = E_{10} = 59{,}400$, $k_{16} = k_{17} = 35$, $n_{16} = n_{17} = 0$, $E_{16} = E_{17} = 38{,}000$, where the rate of the direct reaction is written in the form $W = T^n \exp(k - E/T)$.

Problem (1.1)-(1.21) was solved numerically with the aid of an implicit finite-difference scheme constructed on the basis of an iteration—interpolation method [17]. In this case for calculating system (1.1)-(1.6) we used the method of [18]. The difference scheme and the computation algorithm were described in [10]. To test the program we carried out comparisons with the results for a hypersonic nonequilibrium air flow at the stagnation point [18]; the results were found to coincide with graphic accuracy.

2. Theoretical Investigation of Thermochemical Degradation Regimes

On the basis of the calculations of the body-flow interaction in the neighborhood of the stagnation point we obtained a physical picture of the process over a broad interval of variation of the surface temperatures. There are three interaction regimes. We will determine the heat flow q_W from the gas phase to the solid $q_w = \sum_{i=1}^{3} q_i$, where $q_1 = \lambda \frac{\partial T}{\partial y}\Big|_{y=0}$, $q_2 = -\sum_{i=1}^{L} J_{iw} h_{iw}$, where $q_3 = -(\rho v)_w h_w$. In Figs. 1 and 2 we have presented certain results obtained for an altitude of 30,000 m, $v_\infty = 7500$ m/sec and $R_N = 0.1$ m as functions of T_W. In Fig. 1: 1) q_W; 2) $q_1 + q_2$; 3) q_3; 1' is the mass erosion rate $(\rho v)_W$, 2' and 3' are the erosion fractions corresponding to the first two of heterogeneous reactions (1.22) respectively, 4' is the erosion fraction associated with the sublimation process (1.23). In Fig. 2 the continuous curves represent the values of the flow component concentrations at the surface of the body. At $750°K \leqslant T_W \leqslant 1200°K$ the increase in $(\rho v)_W$ is predetermined by the increase in T_W and the interaction takes place in the kinetic ablation regime.

In the diffusion regime, which in the variant considered corresponds to $1250°K \leqslant T_W \leqslant 3250°K$, the quantity $(\rho v)_W$ is almost constant and is principally determined for given p_e and R_N by the concentration of the oxidizing component. Curves 2' and 3' in Fig. 1 illustrate the contribution of the heterogeneous reactions to the erosion in the kinetic and diffusion regimes. As an analysis shows, the main fraction corresponds to the reaction $C_T + O \rightarrow CO$, the reaction $C_T + O_2 \rightarrow 2CO$ corresponding to not more than 7% of the total mass erosion. Curves 10 and 5 in Fig. 2 illustrate the constancy in the diffusion regime of the concentrations of the principal oxidizing component O and the product of the heterogeneous reactions CO. As T_W increases, there is a sharp fall in CO_2 concentrations, both at the surface of the body and in the flow.

On the interval $3300°K \leqslant T_W \leqslant 3700°K$ we observe a reorganization of the chemical reaction regime as a result of sublimation of the components C, C_2, and C_3 from the surface (see curves 7-9 in Fig. 2). The mass sublimation rate increases from 0 ($T_W \approx 3250°K$) to value equal to $(\rho v)_W$ (see curves 1' and 4' in Fig. 1 at $T_W > 3700°K$). There is a rapid fall in the concentrations of N_2, O_2, CO, O, NO (curves 1-4, 10 in Fig. 2) as T_W increases. At first, the quantity c_{wN}

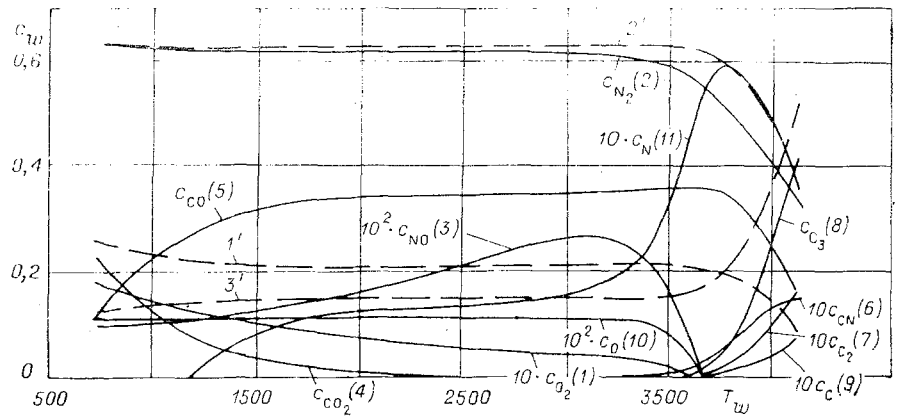

Fig. 2

increases as a result of the intensified dissociation of N_2, and then with increase in $(\rho v)_w$ at $T_w > 3750°K$ it falls. The sublimation regime is associated with a considerable increase in the concentrations of C, C_2, C_3 and CN at the surface; in this case the graphite sublimation fraction in the form C_3 is the greatest. Whereas in the kinetic and diffusion regimes an increase in T_w leads to a slow, almost linear decrease in q_w and for these regimes $q_3 \cong 0$, i.e., $q_w \cong q_1 + q_2$, in the sublimation regime q_3 rapidly increases in absolute value (see curve 3' in Fig. 1), which ensures that the total heat flux falls rapidly to zero. Thus, in the sublimation regime we get thermal shielding as a result of thermochemical degradation. We note that in this regime the effect of injection is also expressed in the hydrodynamic displacement of the boundary layer at the surface and a more rapid fall in the value of $q_1 + q_2$ with increase in T_w as compared with the diffusion regime (curve 2 in Fig. 1). The variation of the element concentrations with T_w is reproduced in Fig. 2: 1') c_O^*; 2') c_N^*; 3') c_C^*. These quantities are almost constant in the diffusion regime and vary considerably in the sublimation regime. We note that according to the results of [7] the value of c_C^* at the surface of the body is equal to 0.15 in the diffusion regime, and that the present calculations give a similar value, namely approximately 0.154.

3. Comparison of the Calculated Thermochemical Degradation Characteristics and the Experimental Data

Comparisons were made with the experimental results of [11, 12]. In order to determine the velocity gradient $du_e/dx|_{x=0}$ we used Newton's equation corrected for moderate Mach numbers and the ratio ρ_∞/ρ_e [19]. We considered three models of the homogeneous chemical reactions: the complete nonequilibrium boundary layer (NBL) model, the "equilibrium" boundary layer (EBL) model, and the "frozen" boundary layer (FBL) model. Table 1 gives values of the erosion rate $(\rho v)_w$ as a function of the temperature T_w, the pressure p at the stagnation point, and the radius R_N given in [11, 12]. Column 4 gives the experimental data of [11, 12], column 5 the theoretical data from [11, 12], columns 6, 8, and 10 the calculations in accordance with the three models mentioned above, the columns 7, 9, and 11 the percentage difference between the $(\rho v)_w$ calculated for the corresponding models and the experimental data. A comparison of the results of the calculations for the NBL model and the experimental data revealed good agreement over the entire interval $2822°K \leqslant T_w \leqslant 3778°K$ as R_N varied from 0.01193 to 0.0363 m. The calculations also showed that at $T_w > 3100°K$ on the interval of R_N in question just as good agreement with the experimental data for $(\rho v)_w$ can be obtained using the EBL model. The agreement is considerably less satisfactory when the FBL model is used, the discrepancy with respect to the experimental data being especially great in the diffusion regime ($T_w \leqslant 3500°K$). In Fig. 3 we have plotted $(\rho v)_w$ against T_w at $p = 0.98 \cdot 10^5$ N/m^2 and $R_N = 0.0184$ m. The points represent the experimental results of [12]; curve 1 corresponds to our data for the NBL model, curves 2-6 to the theoretical results of [12]. There is good agreement between our results and the experimental data not only in the diffusion regime, where the other models proposed in [12] are also reliable, but also in the sublimation regime, where other calculation models either overestimate or underestimate the rate of increase of the erosion rate with T_w. In [12] it was noted that at $T_w > 3700°K$ the quantity $(\rho v)_w$ doubles with increase in T_w by 110°K; our calculations gave the same result for increase in T_w by about 115°K. We note that a sufficiently accurate quantitative description of the erosion in the sublimation regime

is particularly important, since much of the graphite is eroded on the temperature interval characteristic of this regime. The agreement of the calculated and experimental data for the more important thermochemical degradation characteristics indirectly justified the choice of α_i and k, n, and E for reactions (9), (10), (16), and (17) from (1.24). Without considering the possibility of using the simpler EBL or FBL model instead of the complete NBL model, we note that as distinct from the results of the studies cited in [12], the results of the calculations for all three models were obtained by taking into account nonequilibrium physicochemical processes at the surface of the graphite proceeding at a finite rate. The good agreement between our calculations and the experimental results, as compared with the models previously considered, suggests the possibility of reasonably accurate mathematical modeling of the thermochemical degradation process over the entire practical range of variation of the surface temperature within the framework of the NBL model proposed.

4. Simplified Mathematical Models of Thermochemical Degradation and Analysis of Their Accuracy

As shown above, taking into account the nonequilibrium physicochemical processes at the surface of the graphite is necessary in order to describe the thermochemical degradation process. With a view to simplifying the model of the gas-phase reactions it is also of interest to compare the principal characteristics of the process as given by the EBL and FBL models with the results obtained using NBL. Table 2 gives the values of q_w for the three models for certain of the variants considered in Sec. 3; here the difference between the q_w for the EBL and FBL models and the q_w for the complete model is given as a percentage. Table 3 gives values of q_w and $(\rho v)_w$ in the neighborhood of the stagnation point of a sphere with $R_N = 0.01$-1.0 m traveling at an altitude of 30,000 m at $v_\infty = 7500$ m/sec for certain T_w; the significance of the percentage error is the same as described above. We will begin by comparing the results for the models NBL and EBL. As an analysis of the data of Table 2 shows, at a pressure $p_e \sim 10^5$ N/m^2 there is a difference in $(\rho v)_w$ for $T_w \leqslant 3000$°K, the erosion rate being greater according to the NBL theory than it is according to EBL. At the same time, the EBL calculations give an exaggerated value of q_w over the entire interval of T_w in question (see Table 2). At $T_w \geqslant 3100$°K the results with respect to $(\rho v)_w$ are similar for both models (see rows 7-25 in Table 1). At $p_e \sim 10^6$ N/m^2 and $R_N = 0.01$ m the error in determining q_w from the EBL model remains considerable at all the T_w considered (see rows 1-3 in Table 3); the value of $(\rho v)_w$ at $T_w = 2700$°K is underestimated by the EBL model (see row 1 in Table 3), while at $T_w = 3500$; 4000°K it coincides with the NBL data (see rows 2 and 3 in Table 3). As the radius increases, the difference in determining q_w and $(\rho v)_w$ decreases (see rows 4-6 in Table 3) and at $R_N = 1.0$ m the values of q_w and $(\rho v)_w$ are fairly similar for both models. In Fig. 4 we have plotted the results of a comparison with respect to q_w and $(\rho v)_w$ for the two-dimensional problem of flow over a sphere with $R_N = 0.1$ m and a given constant surface temperature in two variants: curves 1-4 for an altitude of 30,000 m, $v_\infty = 7500$ m/sec, $T_w = 3500$°K, curves 5-8 for an altitude of 25,000 m, $v_\infty = 7500$ m/sec, $T_w = 3700$°K. The continuous curves represent the ratios of the heat fluxes q_w for the EBL (curves 1, 5) and FBL (curves 2, 6) models to the q_w data for the NBL model; the dashed curves represent the analogous ratios with respect to $(\rho v)_w$: curves 3, 7 for the EBL model and curves 4, 8 for the FBL model. The pressure distribution over the sphere was taken in accordance with Newton's equation. As follows from an analysis of the graphs, the difference in heat fluxes is the more significant, and at $\theta = 50°$ reaches 25% of EBL. Thus, calculations in accordance with the EBL model may give a substantial difference as compared with the complete model with respect to the characteristics of the process at the stagnation point on a certain real interval of the parameters of the flow and the body, and also give a difference in $(\rho v)_w$ and q_w

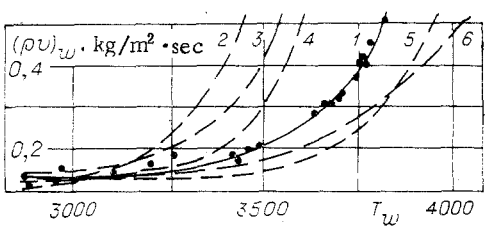

Fig. 3

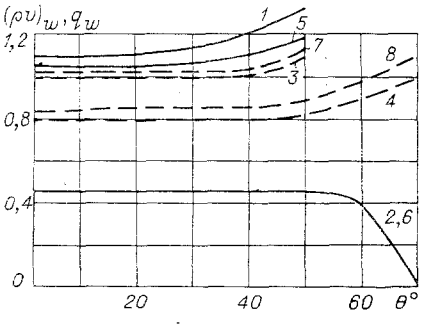

Fig. 4

TABLE 1

T_w, K	$p \cdot 10^{-5}$, N/m²	$R_N \cdot 10^2$, m	$(\rho v)_w$, kg/m²·sec	$(\rho v)_w$	$(\rho v)_w$ (NBL)	%	$(\rho v)_w$ (EBL)	%	$(\rho v)_w$ (FBL)	%
1	2	3	4	5	6	7	8	9	10	11
1 2822	1,03	1,63	0,150	0,145	0,162	7	0,127	16	0,113	25
2 2875	0,99	1,75	0,146	0,137	0,157	8	0,130	11	0,109	25
3 2911	1,03	1,78	0,145	0,138	0,157	8	0,137	5	0,110	24
4 2944	1,09	1,57	0,172	0,151	0,164	5	0,153	11	0,120	31
5 2992	1,06	1,69	0,152	0,145	0,164	8	0,153	1	0,114	25
6 3067	1,06	3,00	0,144	0,108	0,128	11	0,128	11	0,091	37
7 3100	1,12	2,87	0,145	0,117	0,137	6	0,136	6	0,095	34
8 3100	1,12	1,52	0,195	0,156	0,177	9	0,177	9	0,124	36
9 3322	0,95	1,76	0,185	0,139	0,164	11	0,170	8	0,120	35
10 3400	1,06	1,95	0,197	0,145	0,177	10	0,176	10	0,132	34
11 3447	1,02	1,66	0,209	0,159	0,188	10	0,197	6	0,152	27
12 3467	1,11	1,62	0,215	0,169	0,203	6	0,212	2	0,165	23
13 3489	1,09	1,69	0,226	0,165	0,203	10	0,210	7	0,170	25
14 3506	1,07	1,88	0,214	0,160	0,195	9	0,206	4	0,169	21
15 3567	0,98	1,88	0,209	0,165	0,213	2	0,228	9	0,200	4
16 3572	1,21	1,76	0,255	0,185	0,236	7	0,252	2	0,214	16
17 3617	1,03	1,98	0,270	0,177	0,243	10	0,256	6	0,241	11
18 3633	1,13	1,89	0,302	0,192	0,265	12	0,280	8	0,263	13
19 3672	1,06	1,92	0,294	0,203	0,303	3	0,313	7	0,313	7
20 3711	1,13	3,63	0,263	0,164	0,274	4	0,275	4	0,290	10
21 3722	0,99	2,20	0,335	0,211	0,362	8	0,360	8	0,388	16
22 3739	0,99	1,36	0,435	0,283	0,475	8	0,475	8	0,517	19
23 3739	1,09	2,06	0,417	0,231	0,399	4	0,396	5	0,428	3
24 3744	1,06	1,19	0,501	0,307	0,505	1	0,509	2	0,546	9
25 3778	1,23	1,92	0,459	0,269	0,491	7	0,479	4	0,534	16

TABLE 2

	T_w, K	$p \cdot 10^{-5}$, N/m²	$R_N \cdot 10^2$, m	q_w, W/m² (NBL)	q_w (EBL)	%	q_w (FBL)	%
1	2822	1,03	1,63	$1,503 \cdot 10^7$	$1,867 \cdot 10^7$	24	$0,952 \cdot 10^7$	37
2	2944	1,09	1,57	$1,491 \cdot 10^7$	$1,890 \cdot 10^7$	27	$0,981 \cdot 10^7$	34
3	3067	1,06	3,00	$1,127 \cdot 10^7$	$1,300 \cdot 10^7$	15	$0,684 \cdot 10^7$	39
4	3400	1,06	1,95	$0,945 \cdot 10^7$	$1,526 \cdot 10^7$	26	$0,703 \cdot 10^7$	26
5	3506	1,07	1,88	$0,960 \cdot 10^7$	$1,419 \cdot 10^7$	48	$0,580 \cdot 10^7$	40
6	3572	1,21	1,76	$0,873 \cdot 10^7$	$1,451 \cdot 10^7$	66	$1,515 \cdot 10^7$	41
7	3633	1,13	1,89	$0,505 \cdot 10^7$	$1,134 \cdot 10^7$	125	$0,236 \cdot 10^7$	53
8	3711	1,13	3,63	$0,162 \cdot 10^6$	$4,706 \cdot 10^6$	300	$-2,016 \cdot 10^6$	1334

TABLE 3

	T_w, K	$10^{-7} \cdot q_w$, (W/m²) (NBL)	$(\rho v)_w$, (kg/m²·sec)·10² (NBL)	q_w (EBL)	%	$(\rho v)_w$ (EBL)	%	q_w (FBL)	%	$(\rho v)_w$ (FBL)	%
				$R_N = 0{,}01$ m							
1	2700	8,19	5,91	10,1	23	3,72	37	4,15	49	4,18	28
2	3500	7,32	6,04	8,84	21	6,20	3	3,61	50	4,45	26
3	4000	3,29	11,7	5,50	67	11,9	2	6,82	100	12,1	8
				$R_N = 0{,}1$ m							
4	2700	2,85	1,93	3,08	8	1,66	20	1,31	54	1,58	18
5	3500	2,58	2,01	2,77	7	2,08	2	1,14	56	1,67	17
6	4000	1,34	4,06	1,63	17	3,91	1	−0,1	108	4,54	15
				$R_N = 1{,}0$ m							
7	2700	0,93	0,62	0,95	2	0,56	7	0,41	55	0,56	10
8	3500	0,04	0,64	0,87	3	0,66	3	0,36	58	0,58	10
9	4000	0,48	0,13	0,51	5	0,13	2	−0,5	110	0,15	16

over the surface of the body for parameters of the process for which at the stagnation point the results given by the HBL and EBL models are very similar.

A comparison of the results with respect to q_w and $(\rho v)_w$ presented in Tables 1-3 for the NBL and FBL models reveals a considerable difference; in this case the q_w for the FBL model

are much lower than the results for NBL. An even greater difference is observed in the determination of q_w and $(\rho v)_w$ on the lateral surface (curves 2, 4, 6, 8 in Fig. 4).

Thus, under the given conditions the EBL model proved to be the more accurate of the two approximate models.

LITERATURE CITED

1. Park, "Effect of atomic oxygen on graphite ablation," Raketn. Tekh. Kosmon., 14, No. 11 (1976).
2. Baker, "Effect of nonequilibrium chemical processes on graphite sublimation," Raketn. Tekh. Kosmon., 15, No. 10 (1977).
3. N. A. Anfimov, "Combustion of graphite in a high-temperature air flow," Izv. Akad. Nauk SSSR. Otd. Tekh. Nauk, Mekh. Mashinostr., No. 5 (1964).
4. V. V. Shchennikov, "Calculation of a laminar boundary on a sublimating surface," Zh. Vysshl. Mat. Mat. Fiz., 1, No. 5 (1961).
5. F. S. Zavelevich, "Combustion of graphite in a chemically equilibrium boundary layer," Izv. Akad. Nauk SSSR, Mekh. Zhidk. Gaza, No. 1 (1966).
6. Kendall and Bartlett, "Solution of the problem of a multicomponent boundary layer by the integral matrix method," Raketn. Tekh. Kosmon., 6, No. 6 (1968).
7. Skala and Gilbert, "Sublimation of graphite at hypersonic speeds," Raketn. Tekh. Kosmon., 3, No. 9 (1965).
8. J. R. Baron and H. Bernstein, "Heterogeneous rate coupling for graphite oxidation," AIAA Paper No. 70-832 (1970).
9. B. V. Alekseev, The Boundary Layer with Chemical Reactions [in Russian], Computer Center Acad. Sci. USSR, Moscow (1967).
10. A. G. Gofman, A. D. Gruzin, and S. I. Pyrkh, "Nonequilibrium multicomponent boundary layer on a sublimating carbon-graphite surface," ChMMSS, Novosibirsk: ITPM Sib. Otd. Akad. Nauk SSSR, 11, No. 6 (1980).
11. J. H. Lundell and R. R. Dickey, "Graphite ablation at high temperatures," AIAA Paper No. 71-418 (1971).
12. Lundell and Dickey, "Ablation of ATJ graphite at high temperatures," Raketn. Tekh. Kosmon., 11, No. 2 (1973).
13. O. N. Suslov, G. A. Tirskii, and V. V. Shchennikov, "Description of chemical equilibrium flows of multicomponent ionized mixtures within the framework of the Navier–Stokes and Prandtl equations," Zh. Prikl. Mekh. Tekh. Fiz., No. 1 (1971).
14. É. A. Gershbein, "Laminar multicomponent boundary layer at high injection rates," Izv. Akad. Nauk SSSR, Mekh. Zhidk. Gaza, No. 1 (1970).
15. V. G. Gromov, "Calculation of the viscous hypersonic flow over a sphere of a gas mixture containing carbon dioxide," Nauchn. Trudy In-ta Mekhaniki MGU, No. 5 (1970).
16. Thermodynamic Properties of Individual Substances [in Russian], Nauka, Moscow, Vol. 1, Book 2 (1978); Vol. 2, Book 2 (1979).
17. A. M. Grishin and V. N. Bertsun, "Iteration-interpolation method and the theory of splines," Dokl. Akad. Nauk SSSR, 214, No. 4 (1974).
18. V. G. Gromov, "Calculation of a laminar boundary layer in the presence of nonequilibrium reactions," in: New Applications of the Method of Nets in Gas Dynamics, No. 1 [in Russian], Moscow State University, Moscow (1971).
19. N. F. Krasnov, Aerodynamics [in Russian], Vysshaya Shkola, Moscow (1971).